Supplementary information

Exploring potential drivers of divergence in tree-ring based temperature reconstructions of NW North America

Marcel Kunz[1], Rob Wilson[2], Emily Reid[2], Eileen Kuhl[3], Jan Esper[1,4]

[1]Department of Geography, Johannes Gutenberg University, 55128 Mainz, Germany

[2]School of Earth and Environmental Sciences, University of St. Andrews, KY16 9AJ, Scotland, UK

[3]Deutscher Wetterdienst (German Meteorological Service), 63067 Offenbach, Germany

[4]Global Change Research Institute of the Czech Academy of Sciences (CzechGlobe), 61300 Brno, Czech Republic

**Corresponding author*

E-mail address: mkunz01@uni-mainz.de (Marcel Kunz)

Tab. S1. Instrumental data used for the analysis.

	BEST	CRU
Tmean	✓	✓
Tmax	✓	✓
Tmin	✓	✓
Precipitation	X	✓
PDSI	X	✓
grid cell size	1°	0.5°
grid cell center NKL	64.5°N 138.5°W	64.25°N 138.25°W
grid cell center CNY	61.5°N 136.5°W	61.25°N 136.75°W

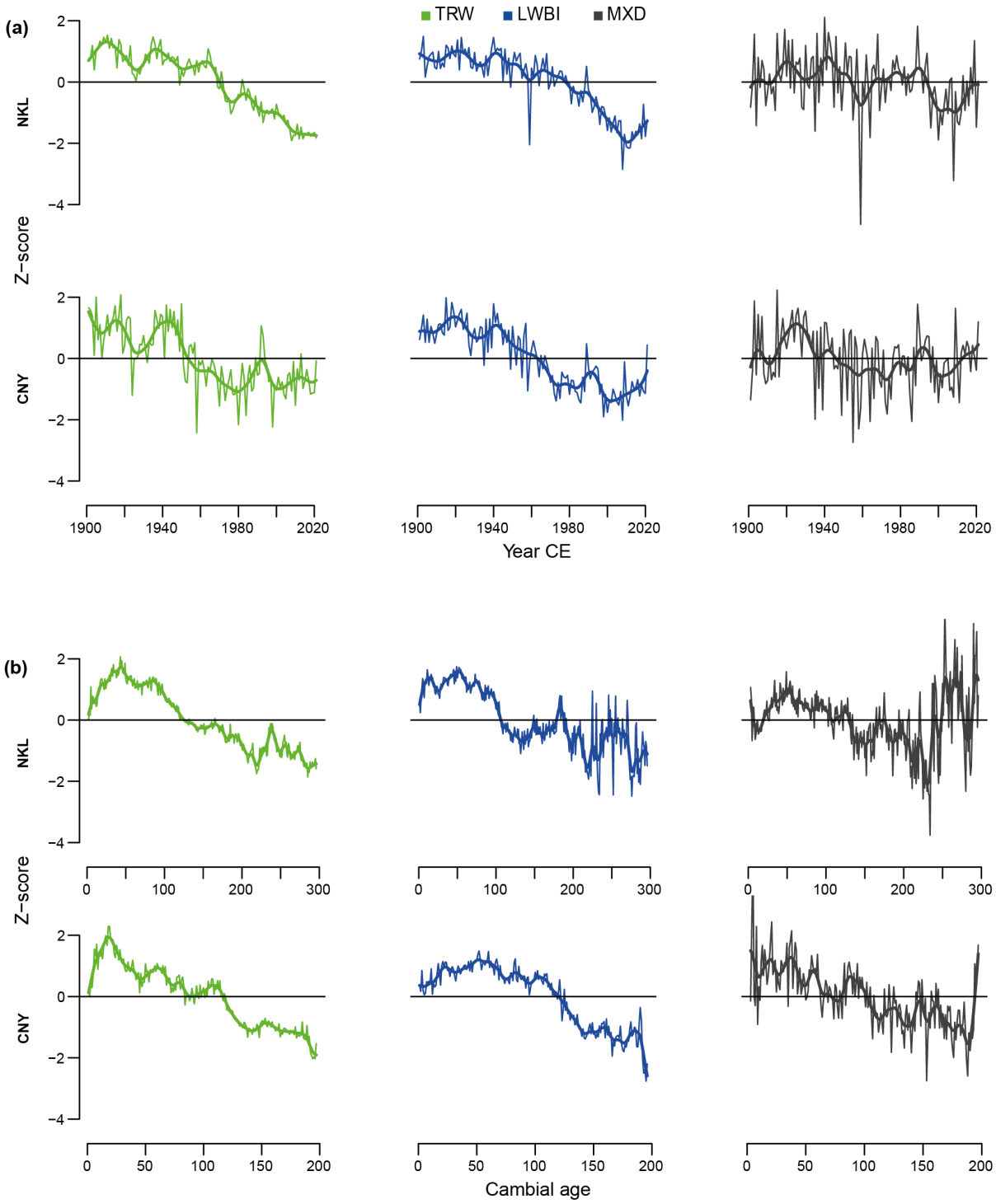

Fig. S1. Undetrended mean chronologies of TR proxies aligned to calendar years **(a)** and cambial age **(b)** for NKL and CNY for the 1901–2021 period.

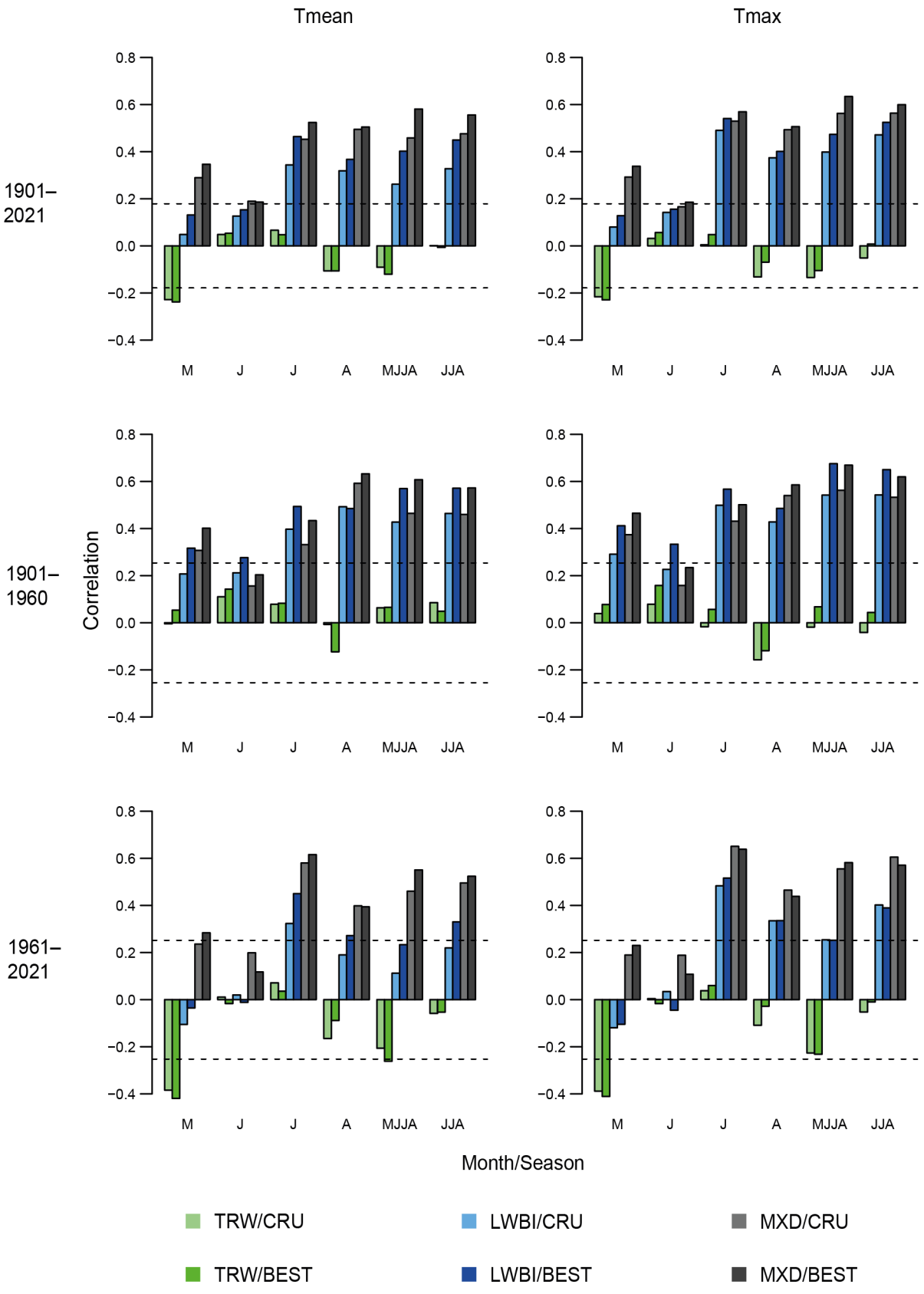

Fig. S2. Correlations between NKL TR proxies and BEST/CRU gridded Tmean and Tmax datasets for the 1901–2021, 1901–1960, and 1961–2021 periods.

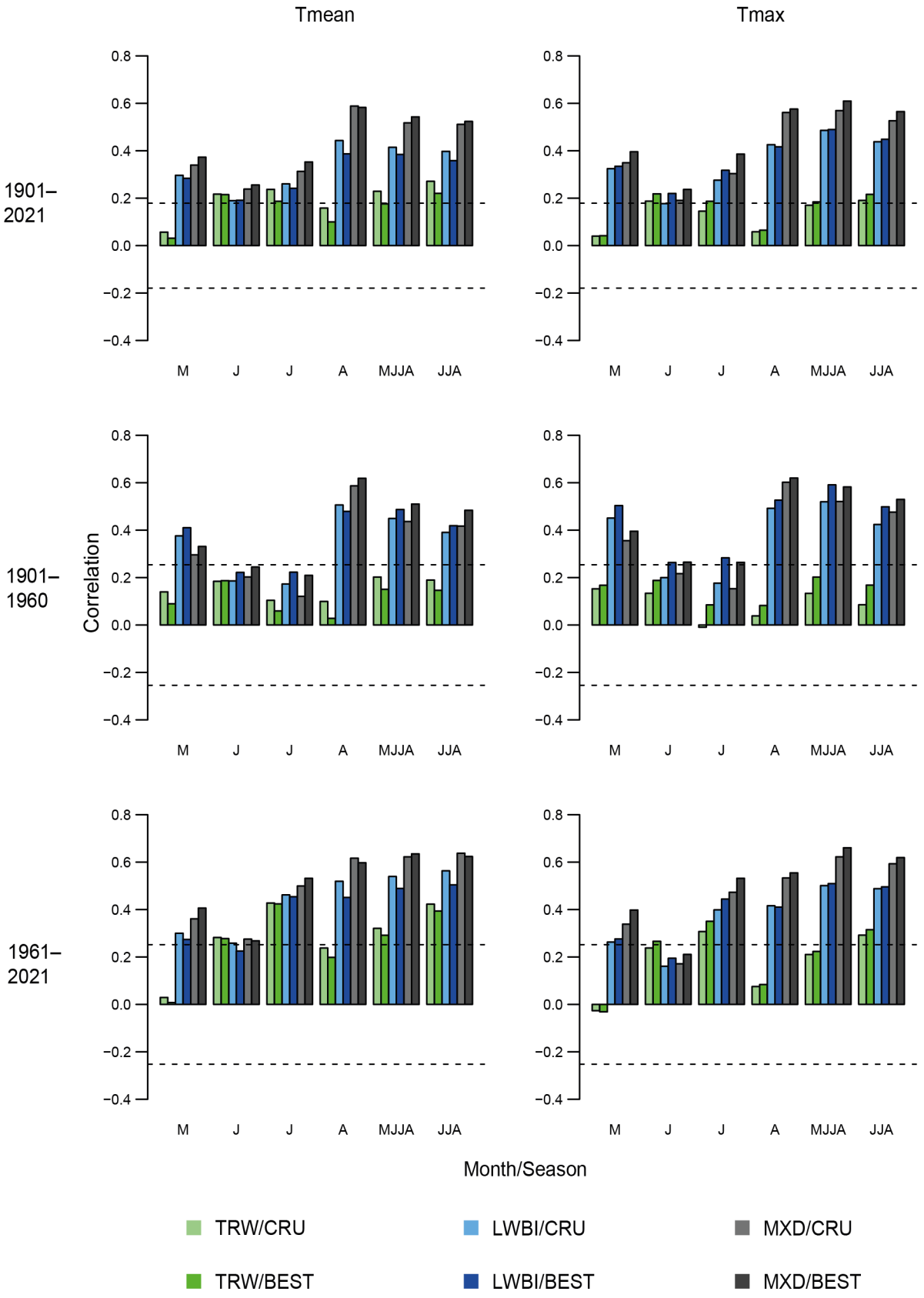

Fig. S3. Correlations between CNY TR proxies and BEST/CRU gridded Tmean and Tmax datasets for the 1901–2021, 1901–1960, and 1961–2021 periods.

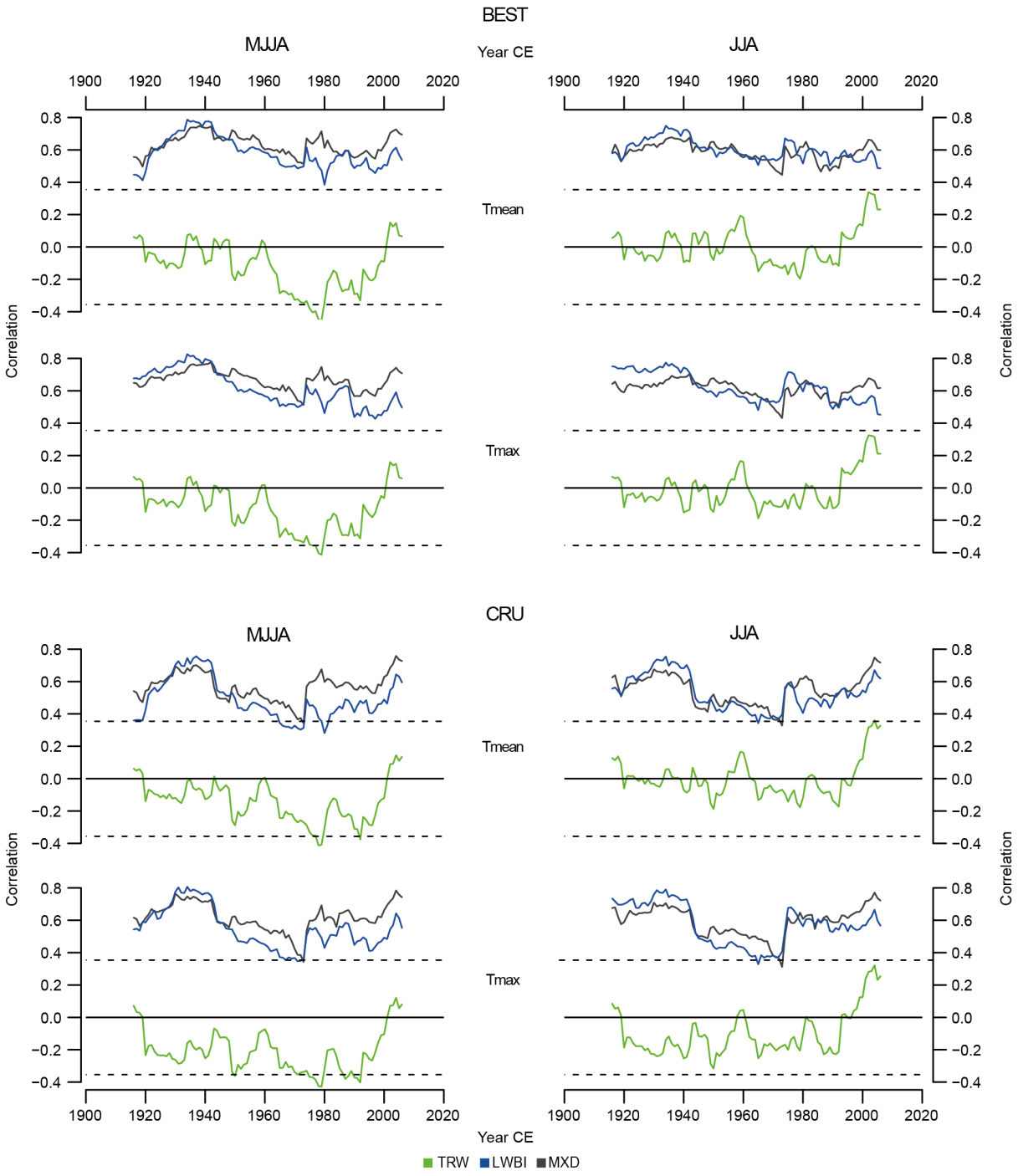

Fig. S4. 31-year moving correlations between NKL TR proxies and BEST/CRU gridded Tmean and Tmax datasets for MJJA and JJA seasons.

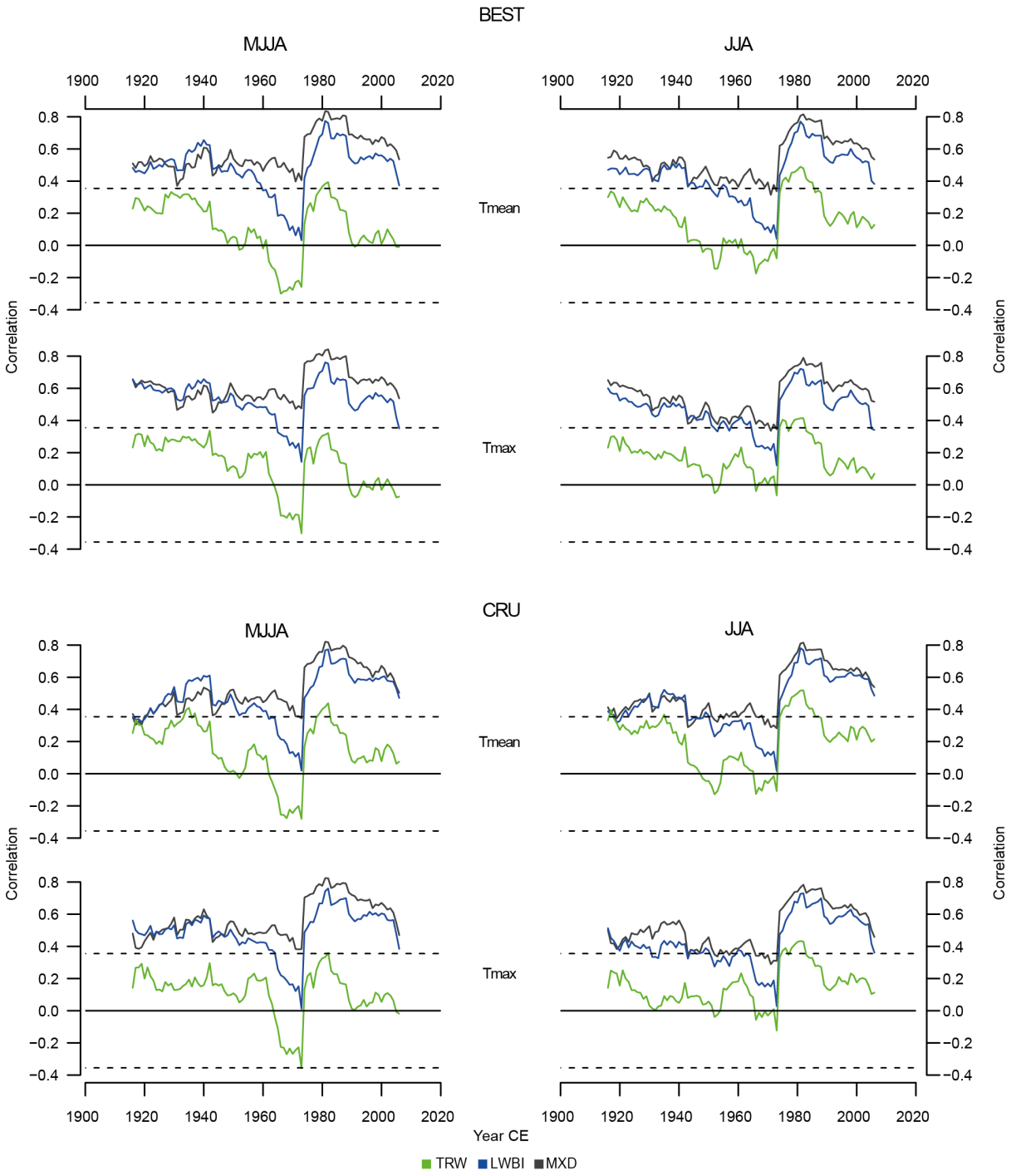

Fig. S5. 31-year moving correlations between CNY TR proxies and BEST/CRU gridded Tmean and Tmax datasets for MJJA and JJA seasons.

Fig. S6. Correlations between TRW and BEST Tmax for previous (p) and current year (c) months and seasons.

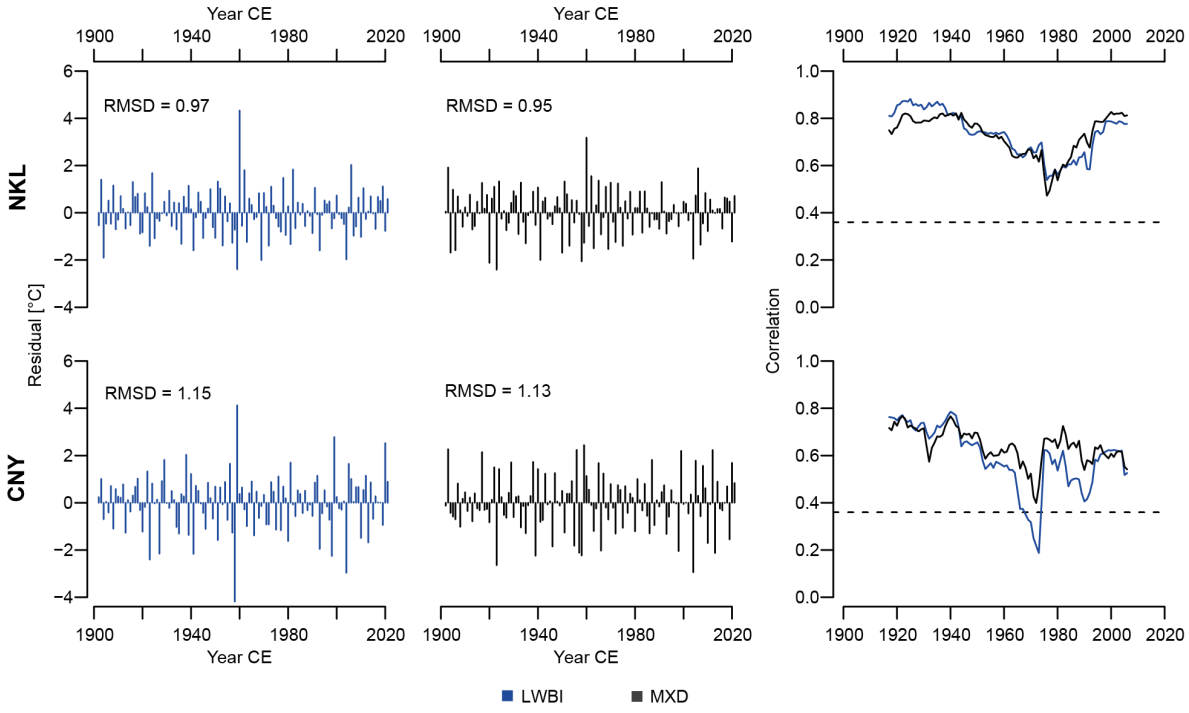

Fig. S7. Annual residuals and 31-year moving correlations between first-difference detrended versions of LWBI/MXD chronologies and May-August Tmax BEST temperatures.

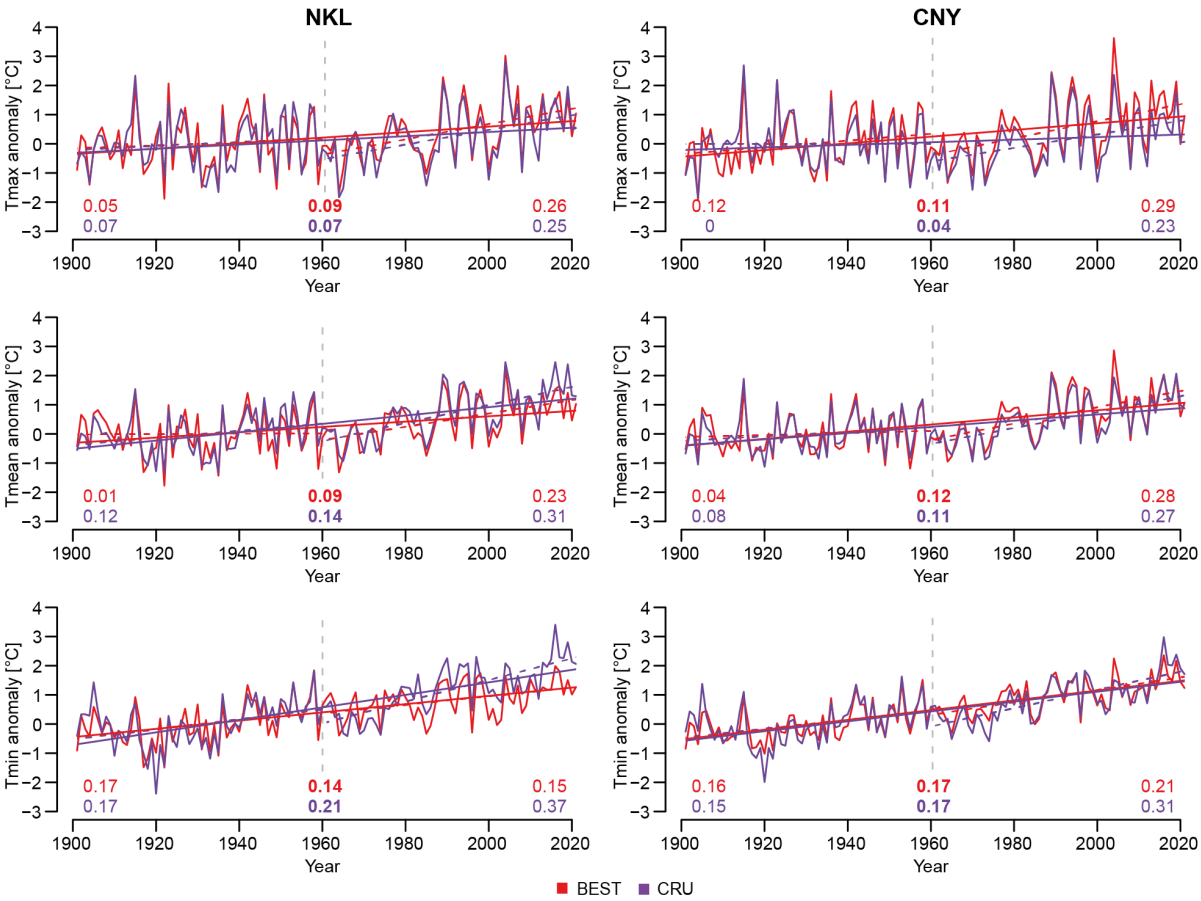

Fig. S8. Tmax, Tmean, and Tmin instrumental CRU and BEST data for the NKL and CNY sites. Solid lines are linear trends for the whole 1901–2021 period and dashed lines for the 1901–1960 and 1961–2021 periods. Central numbers are linear changes across 1901–2021, left and right numbers across the 1901–1960 and 1961–2021 periods.

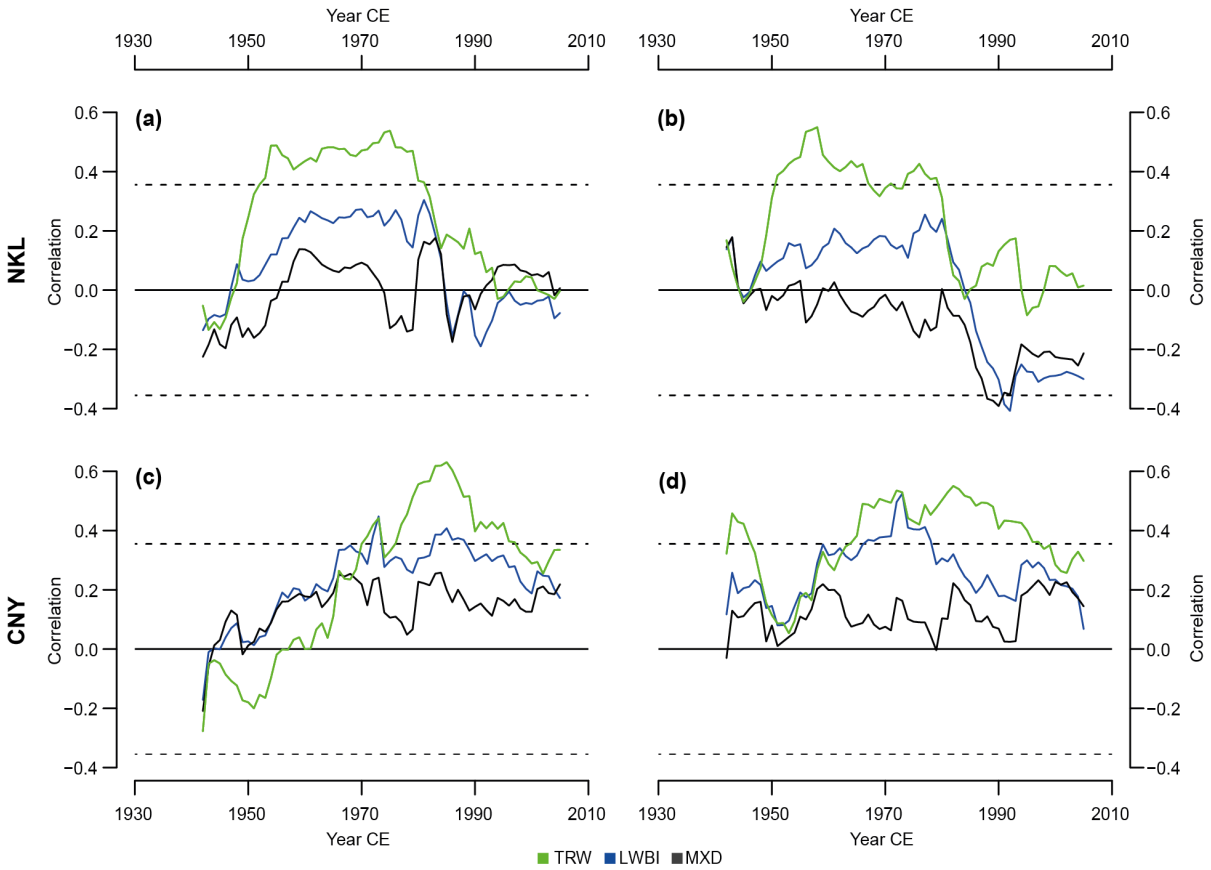

Fig. S9. 31-year moving correlations between tree-ring proxies and precipitation **(a, c)** and self-calibrated Palmer drought severity index **(b, d)** of NKL and CNY for previous to current summer (July–June). Dashed lines indicate significance thresholds for $p<0.05$.

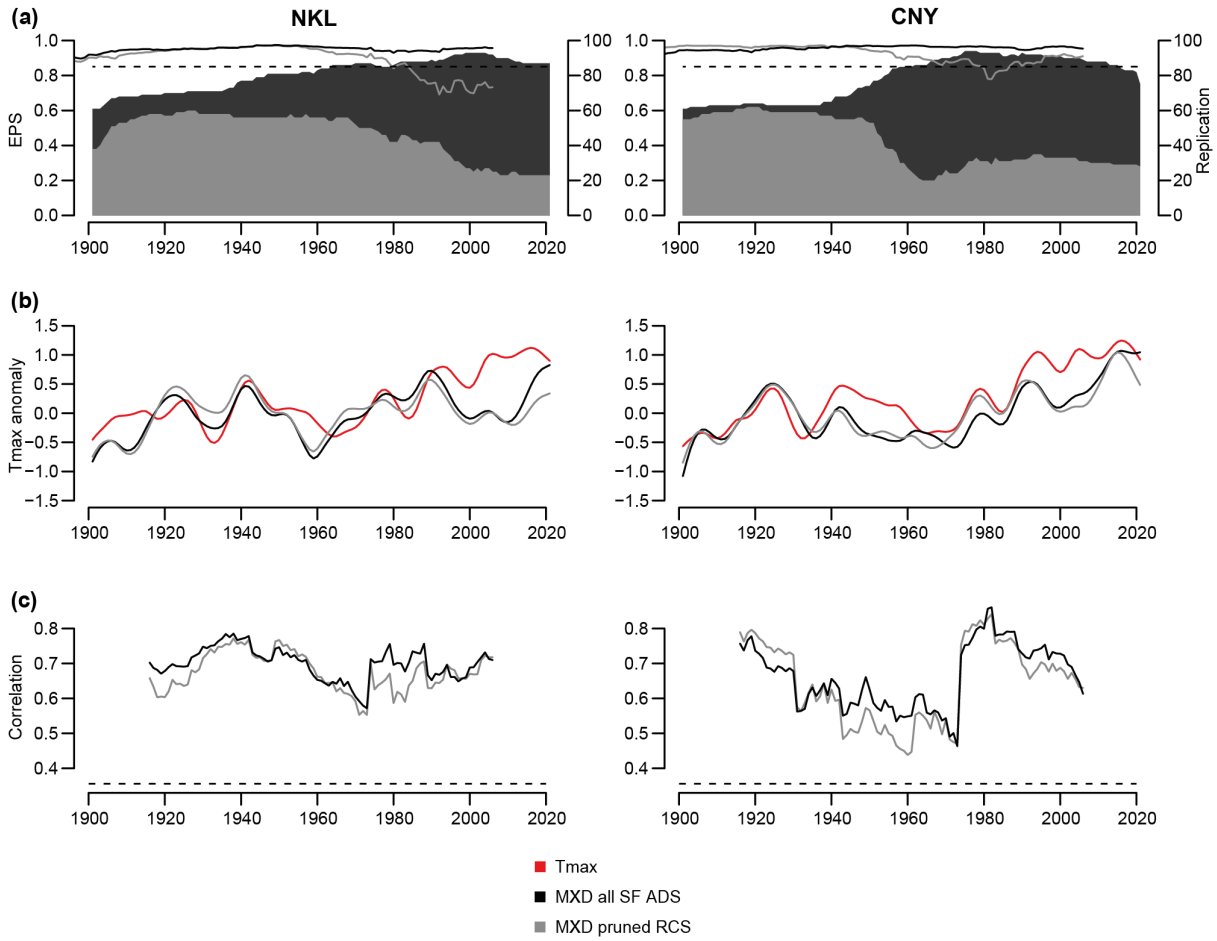

Fig. S10. Comparison between complete, SF ADS-detrended (black) and pruned, RCS-detrended MXD (grey) chronologies of NKL and CNY. **(a)** shows sample replication, 31-year running EPS (solid lines), and 0.85 as a threshold for sufficient EPS (dashed lines). **(b)** are scaled (1901–1960) MXD and May–August Tmax anomaly chronologies and **(c)** 31-year moving correlations between MXD and Tmax with the dashed line indicating the significance threshold for $p<0.05$.

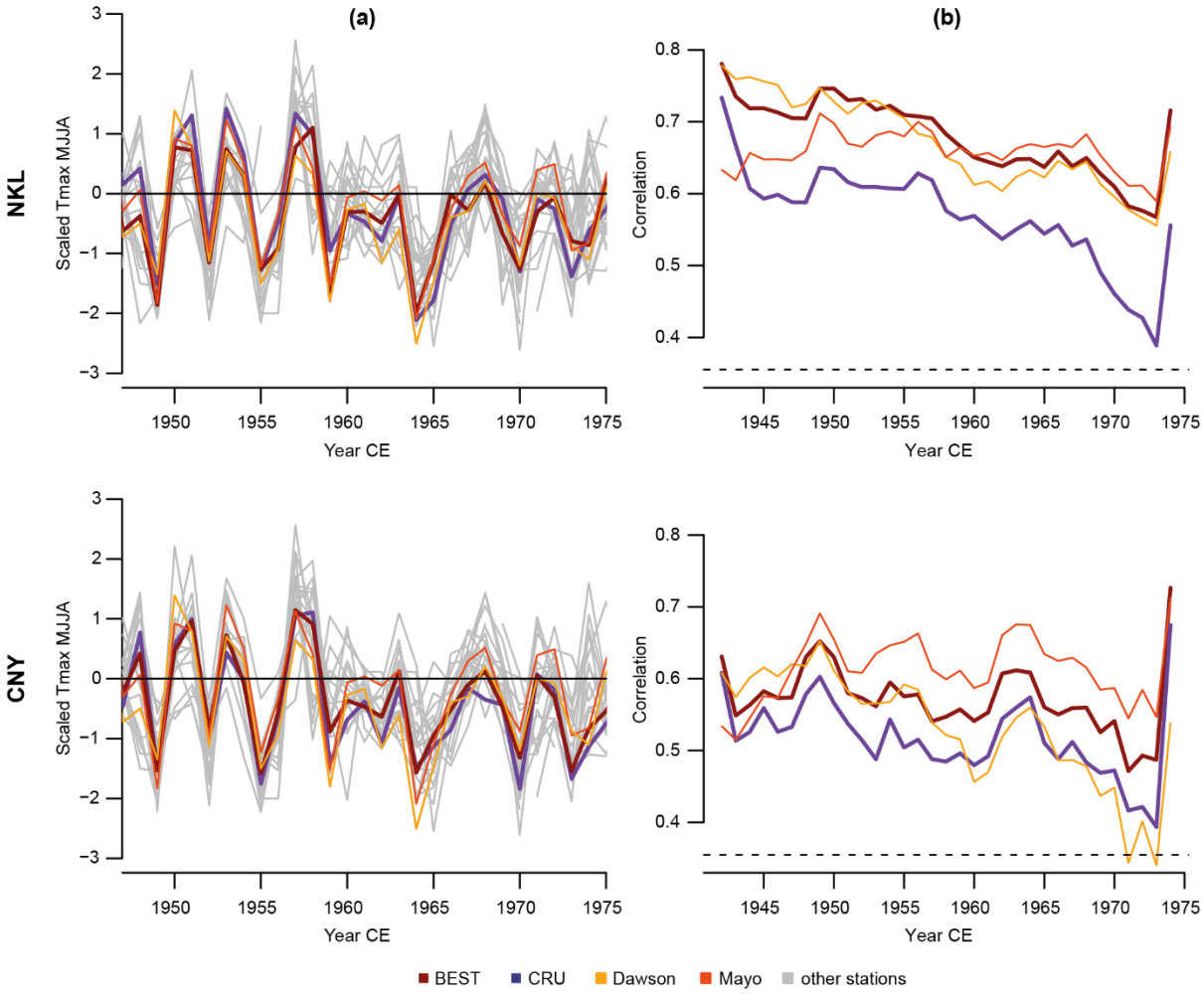

Fig. S11. Gridded (bold lines) and single station (thin lines) May-August Tmax for the period of highest station coverage (1948–1974) **(a)** and 31-year moving correlations between May–August Tmax and MXD for the two gridded and the two most suitable single stations records **(b)**.

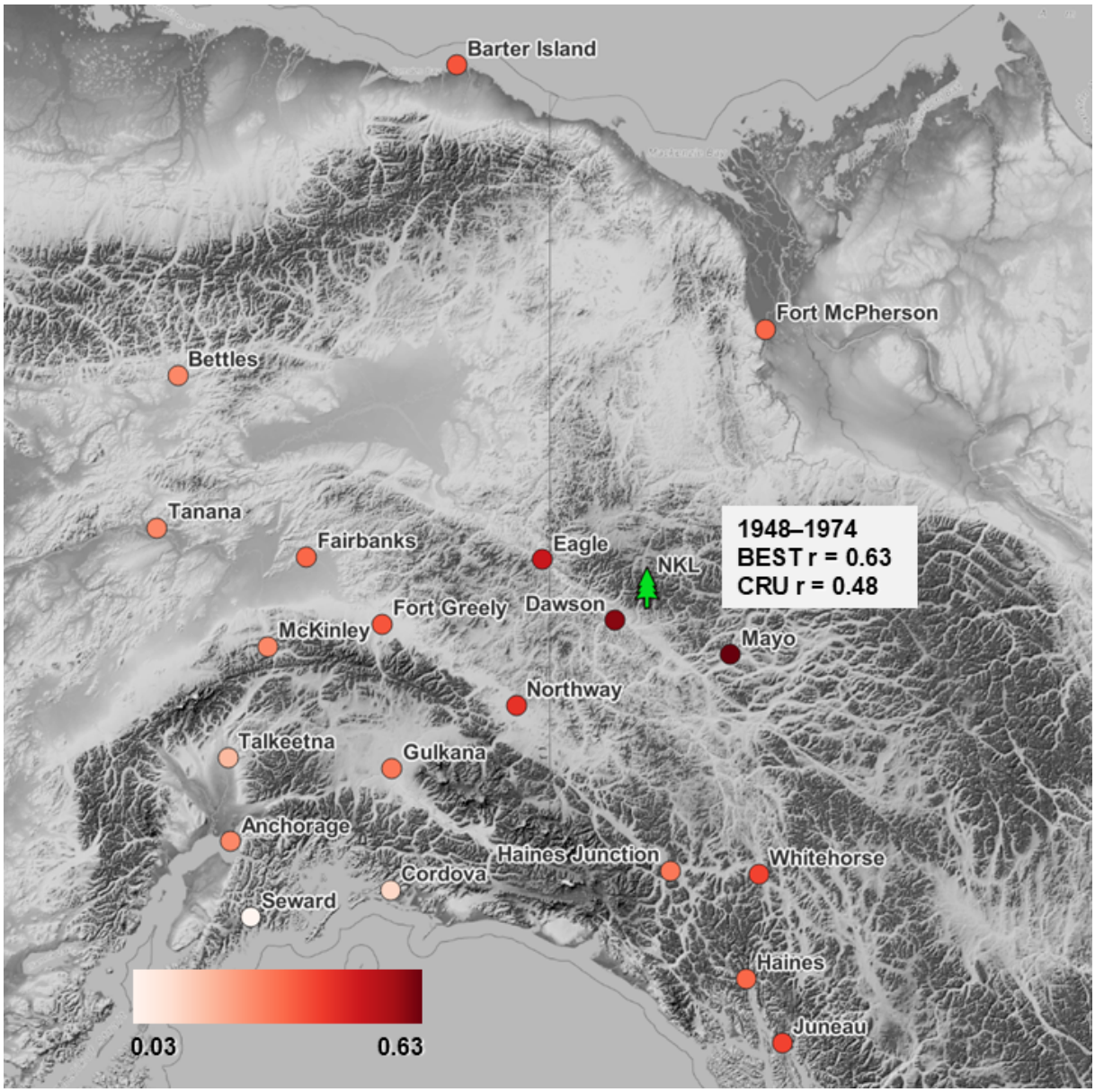

Fig. S12. Correlations between single station May-August Tmax and NKL MXD for the period of highest station coverage (1948–1974).

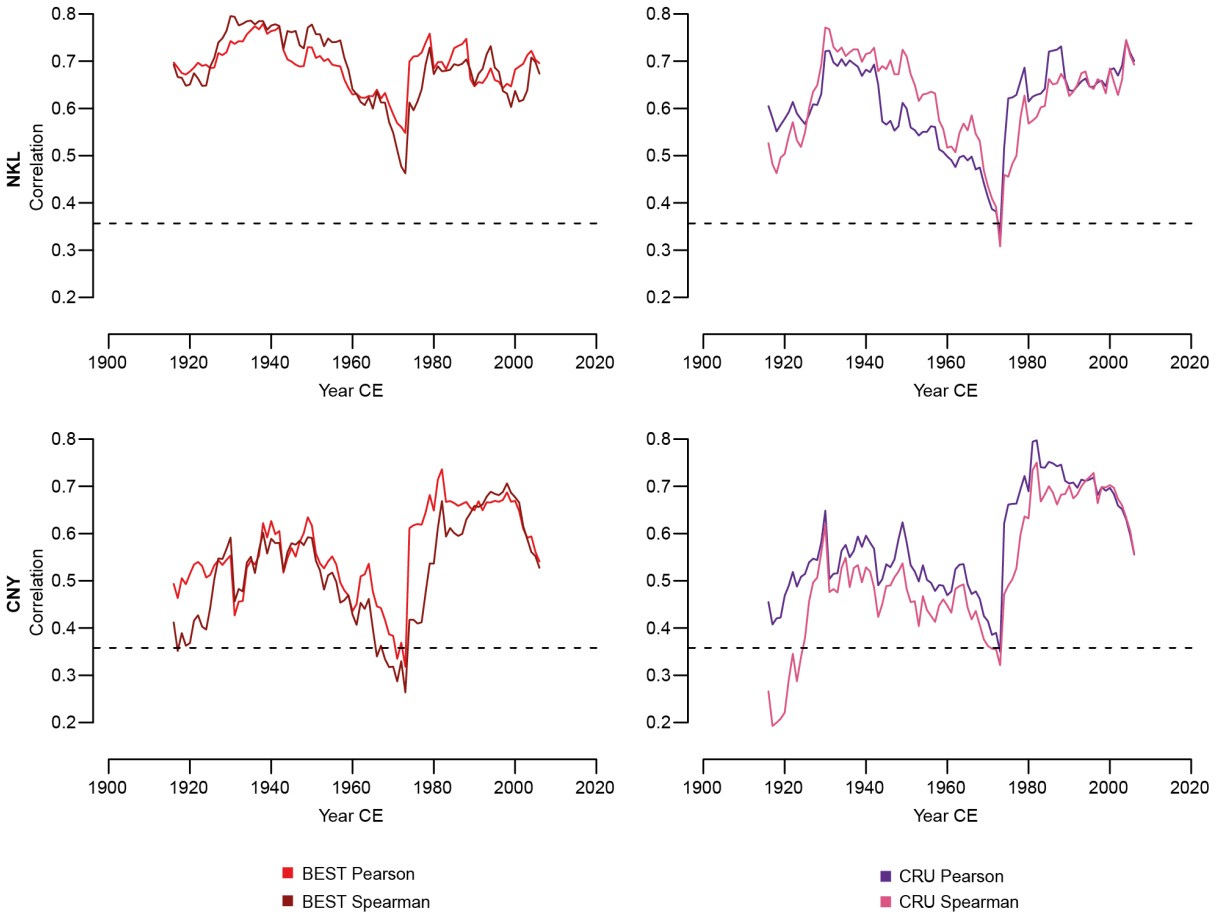

Fig. S13. 31-year moving Pearson and Spearman correlations between MXD and gridded May-August Tmax.

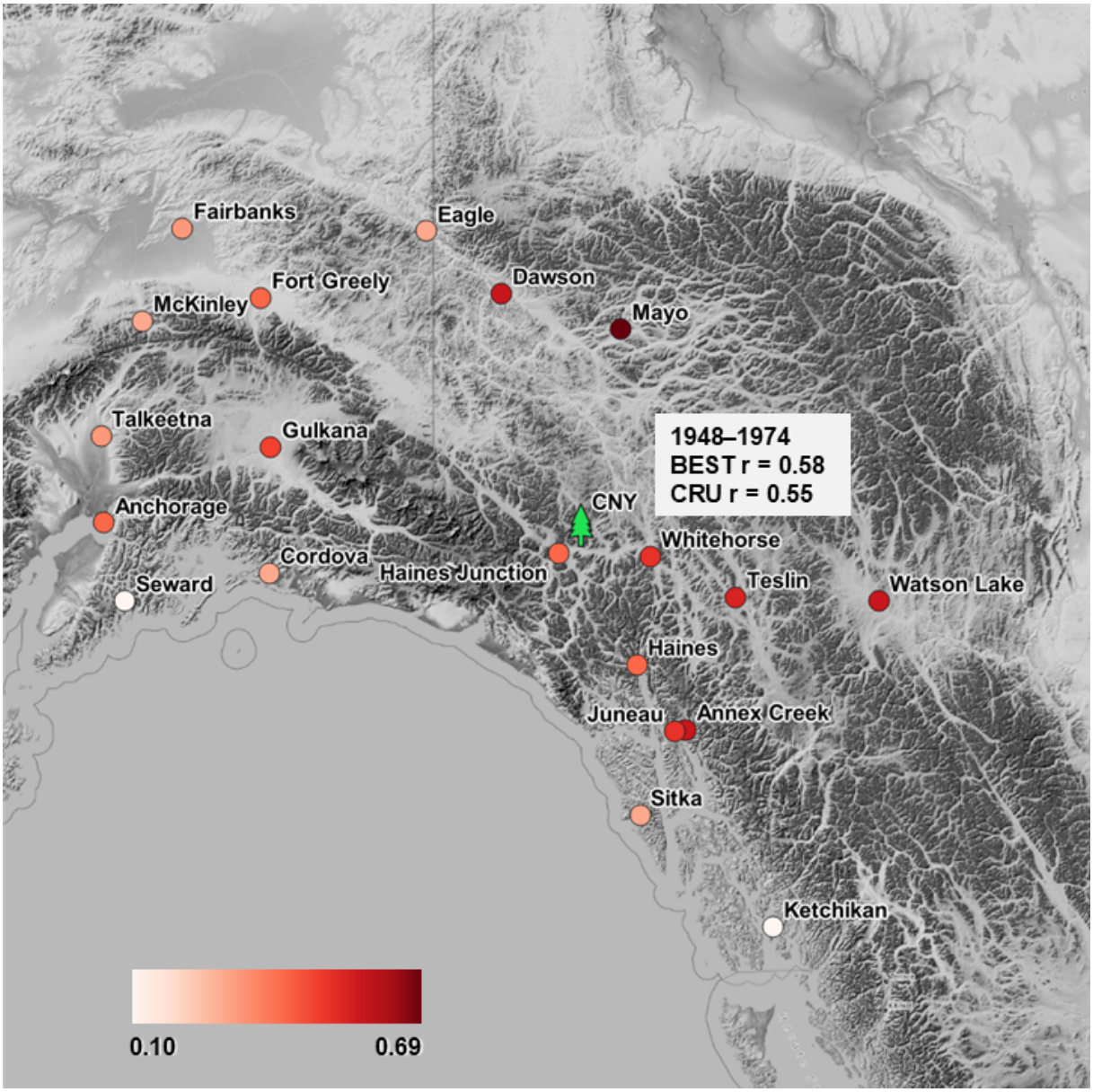

Fig. S14. Correlations between single station May-August Tmax and CNY MXD for the period of highest station coverage (1948–1974).

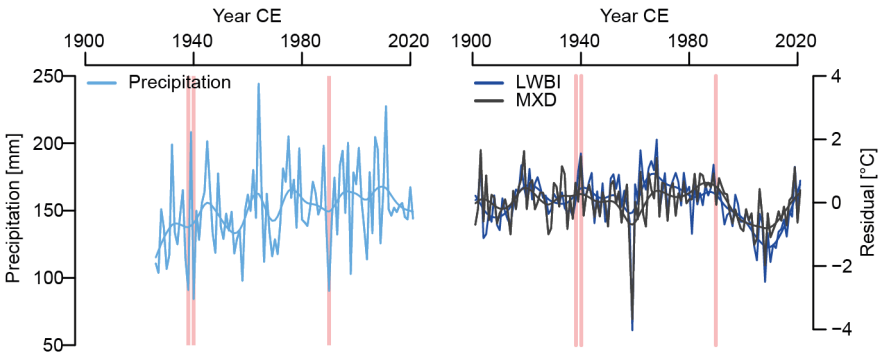

Fig. S15. Spring and early summer precipitation (March–July) at NKL with red bars indicating 1938, 1940, and 1990 as the three driest years and residuals between May–August Tmax and proxy chronologies scaled over the whole period.